Paper

Gas Flow Simulation in GCB Chambers Featuring Hot Gas Energy

Tadashi Mori* Member
Katsuharu Iwamoto* Non-member
Hiromichi Kawano* Member
Yasunori Tanaka** Member

A hot gas simulation in self-blast type GCBs was performed and revised. As a result, it was foundto be important to consider the thermodynamic and transport properties of SF_6-PTFE gas at high pressures and temperatures. Moreover, modelling arc diameters are also important in the chamber. They have become the main factors in determining the rise of puffer pressure in self-blast type GCBs, while they were not relevant in conventional puffer-type GCBs.

Keywords: gas circuit breaker, gas flow simulation, thermodynamic and transport property, self-blast

1. Introduction

Gas circuit breakers (GCBs) filled with SF_6 gas have been adopted for power transmission systems, especially in conditions with high voltages and high interruption currents, due to their novel dielectric and arc extinguishing abilities. Puffer types of SF_6 GCB have been developed up to 550 kV–63 kA per break. Gas flow simulations have been adopted to develop such GCBs. Simulations have been carried out to evaluate temperature, density, and pressure in the arcing area between contacts, as well as in the area between enclosed tank and chambers [(1)(2)]. Such simulations have helped researchers and designers to predict the performance of chambers prior to interrupting tests, which has saved time and costs for developments.

Recently, a new type of chamber called a self-blast type chamber, which does not use mechanical compression to blast gas in current interruptions has been developed [(3)]. However, the authors have found that gas flow simulations that agree well with experimental results in puffer-type chambers could simulate only less puffer pressure in the self-blast type.

This paper describes investigations on obtaining a reasonable puffer pressure in gas flow simulations of a self-blast type chamber. The simulation methods have been developed using a gas flow simulation code called modified FLuid In Cell (FLIC) [(1)(4)(5)]. Although well-developed simulation methods are used by many researchers [(6)(7)], development of FLIC has been placed emphasis on constructing an engineering tool that is easy to simulate and does not take too much time. Historically, the thermodynamic and transport properties of SF_6 gas at a gas pressure below 1.62 MPa (16 atm in literature) have been referred to in literature [(8)–(10)]. The properties of pure SF_6 gas in regions up to 10 MPa and 30000 K have already been reported and have been adopted in FLIC [(7)]. However, the thermodynamic and transport properties of SF_6-Polytetrafluoroethylene (PTFE) mixed gas have not been reported for high-pressure and high-temperature regions. Expecting a key-point in simulating self-blast type chambers, properties up to 10 MPa and 30000 K were obtained and were adopted in hot gas flow simulations in this paper. Moreover, arcs were modelled as grids of resistors to simulate changes of arc diameters.

* Toshiba Corporation
2-1, Ukishima-cho, Kawasaki-ku, Kawasaki 210-0862
** Kanazawa University
2-40-20, Kodatsuno, Kanazawa 920-8667

2. GCB Chamber

In this paper, simulations focus on self-blast type chambers. Fig. 1 is a schematic figure of a self-blast type chamber. This type of chamber generates high pressures by taking hot gas into a thermal puffer chamber from high current arcs, and blasts the high-pressure gas to the arcing area at around current zero. Although the chamber has a mechanical compressive puffer to interrupt small currents, the gas in the mechanical puffer is diffused from relief valves and does not contribute to high current interruptions. Therefore, the mechanical puffer was omitted in simulations shown in this paper.

3. Calculations of Thermodynamic and Transport Properties of SF_6-PTFE Gas

The thermodynamic and transport properties of SF_6-PTFE mixed gas up to 10 MPa and 30000 K were used in the FLIC-D described in section 4. This section outlines the calculation methods for the properties followed by their results. Details

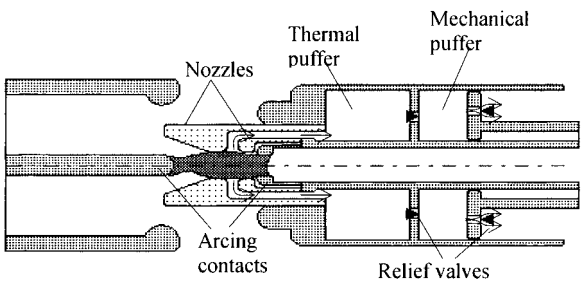

Fig. 1. Schematic figure of a self-blast type chamber

Table 1. Considered particles in SF_6-PTFE gas

	Originate from SF_6	Originate from PTFE
Molecules	SF_6, SF_5, SF_4, SF_3, SF_2, SF, SSF_2, FSSF, F_2, S_2	C_2F_6, C_2F_4, C_2F_2, CF_4, CF_3, CF_2, CF, CS_2, CS, C_5, C_4, C_3, C_2
Atoms	F, S	C
Ions	F-, F+, S+, F_2^+, S_2^+, S^-, S_2^+, F_2^+, SF^+, SF^-	CF_3^+, CF_2^+, C^+, C^-, C_2^+, CS^+, C_2^-, C_2^-
Electrons	e^-	

of the methods can be referred to in the literature [11][12].

3.1 Calculation Methods Table 1 shows the particles considered in the calculation. In addition to electrons, 22 kinds of particle originated from SF_6 gas, and another 22 from PTFE gas. Basic equations relating dissociation and ionise reaction for these particles were solved by the Newton-Raphson method. Equilibrium compositions of SF_6-PTFE mixed gas at various pressures were obtained. Using the results of gas composition, the properties in high-pressure and -temperature gas with a mixture of related molecules, atoms, ions, and electrons were calculated.

Gas constant R

Gas constant R is defined as Eq. (1) using mass density ρ.

$$R = p/\rho T \cdots\cdots (1)$$

where, T is temperature, p is pressure and ρ can be calculated as Eq. (2).

$$\rho = \sum_{i=1}^{N} m_i n_i \cdots\cdots (2)$$

where, m_i is mass of particle i, n_i is density of particle i, and N is the number of specimens considered in the calculations.

Enthalpy h

Enthalpy h was obtained by Eq. (3).

$$h = \frac{1}{\rho}\sum_{i=1}^{N} h_i m_i n_i \cdots\cdots (3)$$

where, h_i is enthalpy of particle i and can be obtained by Eq. (4).

$$h_i = \frac{1}{m_i}\left(\frac{5}{2}kT + kT^2\frac{\partial}{\partial T}(\ln Z_i) + \Delta_f H_i^0\right) \cdots\cdots (4)$$

where, k is Boltzmann constant, Z_i is the internal partition function of particle i. In the equation, $\Delta_f H_i^0$ is a standard enthalpy of formation, which is the reaction heat produced from composition elements in a standard state of 0 K and 0.1 MPa.

Specific heat ratio γ

Specific heat ratio γ can be obtained as follows.

$$\gamma = \frac{C_p}{C_v} = \frac{C_p}{C_p - R} \cdots\cdots (5)$$

$$C_p = \left.\frac{\partial h}{\partial T}\right|_{p=const} \cdots\cdots (6)$$

where, C_p is isopiestic specific heat. The transport properties were calculated using formulas given by Yos, based on the first-Chapman-Enskog approximation [13].

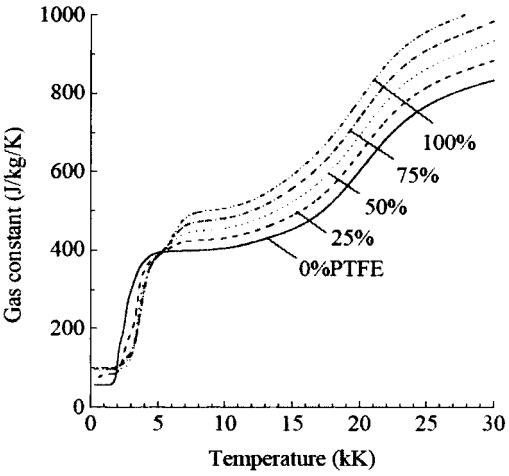

Fig. 2. Gas constant R of SF_6-PTFE at a pressure of 1 MPa for different mixture ratios

Electrical conductivity σ

Electrical conductivity σ was calculated by Eqs. (7) and (8).

$$\sigma = \frac{e^2}{kT}\frac{n_e}{\sum_{\substack{j=1\\ j\neq e}}^{N} n_j \Delta_{ij}^{(1)}} \cdots\cdots (7)$$

$$\Delta_{ij}^{(1)} = \frac{8}{3}\left(\frac{2m_i m_j}{\pi kT(m_i+m_j)}\right)^{1/2}\overline{\pi\Omega_{ij}^{(1,1)}} \cdots\cdots (8)$$

where, $\overline{\pi\Omega_{ij}^{(1,1)}}$ is the momentum transfer collision integral.

Thermal conductivity κ

Thermal conductivity κ was calculated using the following equations.

$$\kappa = \kappa_{tr} + \kappa_{\rm int} + \kappa_{re} \cdots\cdots (9)$$

$$\kappa_{tr} = \frac{15}{4}k\sum_{i=1}^{N}\frac{n_i}{\sum_{j=1}^{N}\alpha_{ij}n_i\Delta_{ij}^{(2)}} \cdots\cdots (10)$$

$$\alpha_{ij} = 1 + \frac{\left(1 - m_i/m_j\right)\left(0.45 - 2.54\cdot m_i/m_j\right)}{\left(1 + m_i/m_j\right)^2} \cdots\cdots (11)$$

$$\Delta_{ij}^{(2)} = \frac{16}{5}\left(\frac{2m_i m_j}{\pi kT(m_i+m_j)}\right)^{1/2}\overline{\pi\Omega_{ij}^{(2,2)}} \cdots\cdots (12)$$

$$\kappa_{\rm int} = k\sum_{i=1}^{N}\frac{\left(C_{pi}M_i/R_{un} - 5/2\right)n_i}{\sum_{j=1}^{N} n_j\Delta_{ij}^{(1)}} \cdots\cdots (13)$$

$$\kappa_{re} = k\sum_{\ell=1}^{N_r}\frac{(\Delta H_\ell/RT)^2}{\sum_{i=1}^{N}(\beta_{\ell i}/n_i)\left\{\sum_{j=1}^{N}(\beta_{\ell i}n_j - \beta_{\ell j}n_i)\Delta_{ij}^{(1)}\right\}} \cdots\cdots (14)$$

where, $\overline{\pi\Omega_{ij}^{(2,2)}}$ is viscosity collision integral, M_i is molecular mass of particles i, R_{un} is universal gas constant (=8.31 J/mol·K), N_r is number of chemical reactions, and $\beta_{\ell i}$ is stoichiometric coefficient in ℓth chemical reaction of particle i. ΔH_ℓ is reaction heat per mol calculated by Eq. (15).

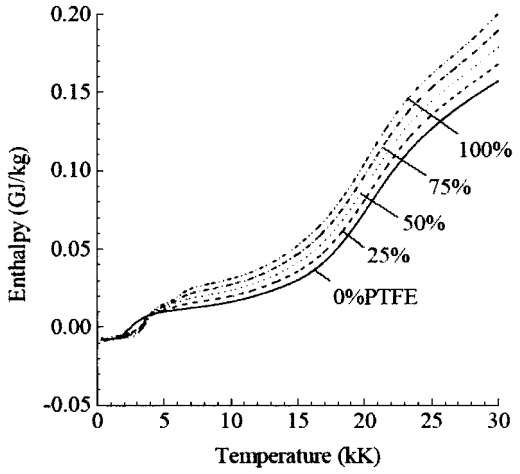

Fig. 3. Enthalpy h of SF_6-PTFE at a pressure of 1 MPa for different mixture ratios

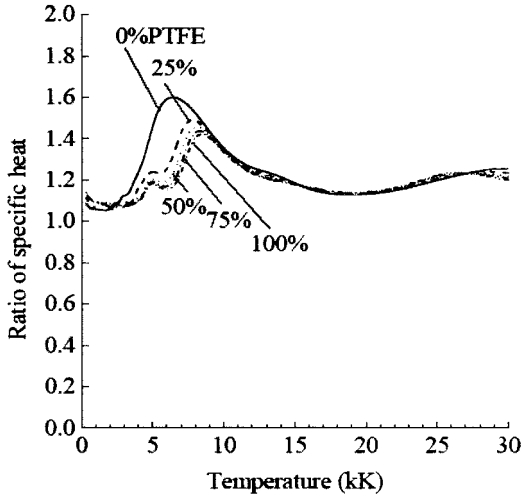

Fig. 4. Ratio of specific heat γ of SF_6-PTFE at a pressure of 1 MPa for different mixture ratios

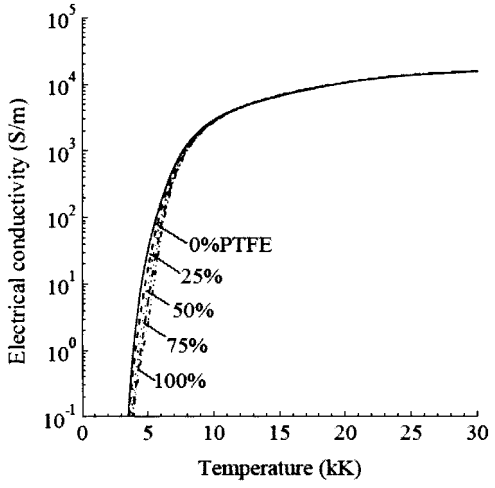

Fig. 5. Electrical conductivity σ of SF_6-PTFE at a pressure of 1 MPa for different mixture ratios

$$\Delta H_i = \sum_{i=1}^{N} \beta_{\ell i} h_i M_i \cdots\cdots (15)$$

3.2 Results of Calculations Figs. 2 to 6 show examples of the calculation results of gas constant R, enthalpy h, specific heat ratio γ, electrical conductivity σ, and thermal conductivity κ, respectively. Each figure indicates the results for PTFE ratios of 0, 25, 50, 75, and 100% at pressures of 1 MPa. Similarly, the results for pressures up to 10 MPa were obtained successfully.

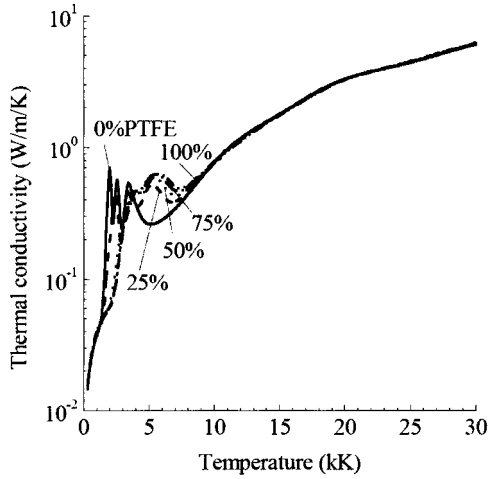

Fig. 6. Thermal conductivity κ of SF_6-PTFE at a pressure of 1 MPa for different mixture ratios

4. Simulation Methods of Gas Flow Simulations

The modified FLIC method developed for GCBs is adopted for hot gas flow simulations in this paper. The modified FLIC introduces non-constructive grids providing a kind of differential method. Overviews of the methods are represented in this section [(1)(6)(7)].

4.1 Fundamental Equations of FLIC Continuous equations, momentum equations for axis and radius directions, and energy conservation equations are described as follows.

Continuous Equations

$$\frac{\partial \rho}{\partial t} + \frac{\partial}{\partial x}(\rho u) + \frac{1}{r}\frac{\partial}{\partial r}(r\rho v) = 0 \cdots\cdots (16)$$

$$\frac{\partial \rho_p}{\partial t} + \frac{\partial}{\partial x}(\rho_p u) + \frac{1}{r}\frac{\partial}{\partial r}(r\rho_p v) = 0 \cdots\cdots (17)$$

$$\frac{\partial \rho_c}{\partial t} + \frac{\partial}{\partial x}(\rho_c u) + \frac{1}{r}\frac{\partial}{\partial r}(r\rho_c v) = 0 \cdots\cdots (18)$$

Momentum Equation for Axis Direction

$$\frac{\partial}{\partial t}(\rho u) + \frac{\partial}{\partial x}(\rho u u) + \frac{1}{r}\frac{\partial}{\partial r}(r\rho u v) = -\frac{\partial p}{\partial x} \cdots\cdots (19)$$

Momentum Equation for Radius Direction

$$\frac{\partial}{\partial t}(\rho v) + \frac{\partial}{\partial x}(\rho v u) + \frac{1}{r}\frac{\partial}{\partial r}(r\rho v v) = -\frac{\partial p}{\partial r} \cdots\cdots (20)$$

Energy Conservation Equations

$$\frac{\partial}{\partial t}(\rho E) + \frac{\partial}{\partial x}(\rho E u) + \frac{1}{r}\frac{\partial}{\partial r}(r\rho E v) = -\frac{\partial}{\partial x}(pu) - \frac{1}{r}\frac{\partial}{\partial r}(rpv) - \kappa\frac{\partial}{\partial x}\left[\frac{\partial T}{\partial x}\right] - \kappa\frac{1}{r}\frac{\partial}{\partial r}\left[r\frac{\partial T}{\partial r}\right] + q_{arc} - q_{rad} - \rho_p E_{pab} - \rho_c E_{cab} \cdots\cdots (21)$$

$$E = \frac{p}{(\gamma-1)\rho} + \frac{1}{2}(u^2 + v^2) \cdots\cdots (22)$$

where, E is energy per mass unit, E_{pab} is ablation energy of PTFE per mass and time unit, E_{cab} is ablation energy of copper per mass and time unit, q_{arc} is inputted thermal energy of an arc per unit volume, q_{rad} is thermal radiation from an arc, r is radius coordinate value, t is time, u is axial velocity, v is radius velocity, χ is axial coordinate, and ρ is density of the mixture gas of SF_6, PTFE, and copper, ρ_p, and ρ_c are densities of PTFE and copper, respectively.

Equation (16) represents the mass balance of the mixture gas of SF_6, PTFE, and copper. Similarly, Eqs. (17) and (18) represent mass balances of PTFE and copper, respectively. p was obtained by the relationship as Eq. (23) derived from Eq. (1).

$$p = \rho RT \cdots\cdots (23)$$

Assuming an arc to be a grey body, thermal radiation of the arc q_{rad} is given by Eq. (24).

$$q_{rad} = \varepsilon B_S \left(T_{arc}^4 - T_{amb}^4\right) S \cdots\cdots (24)$$

where, T_{arc} is arc temperature, T_{amb} is temperature of surrounding area, S is surface area, ε is radiation ratio, and B_S is Stephan-Boltzmann constant (5.6687×10^{-8} W/m^{2}K^4). T_{amb} corresponds to the temperature of the nozzle wall surface because the arc burns within a nozzle.

4.2 Applied Methods Four revisions of the FLIC are compared in this paper with the following features.

(1) FLIC-A Arc energy is given by multiplying arc current and average arc voltage, which was specified by referring to experimental measured values in similar cases. The ablated PTFE and copper, which are materials of nozzles and arcing contacts, are represented as masses appearing on the surfaces of nozzle walls or electrodes [6]. The total amounts of ablated materials were estimated from experimental results. Thermodynamic and transport properties of pure SF_6 gas up to a pressure of 10 MPa and a temperature of 30000 K were adopted [7]. The program had the values in tables, and derived corresponding values at each mesh.

(2) FLIC-B In addition to FLIC-A, the thermodynamic and transport properties of SF_6 gas in the arcing area were multiplied by constants to model 100% of PTFE gas. The multiplied constants were determined for 0.1 MPa from literature [9][14], and the same values were used for other pressures. Here, the assumption of 100% PTFE might be higher than that of actual phenomena, but literature [15] suggests that it could not be so great in high current conditions.

(3) FLIC-C In addition to FLIC-B, the electrical conductivity of the arcs was derived at every mesh in the arcing area. The meshes in the arcing area were modelled as grids of resistors, and arc current was distributed among parallel meshes in inverse proportion to resistance. The arcing energy in each mesh was calculated as Joule heat energy in each resistor. The current could concentrate in meshes along the axis, and arc diameters could be smaller under lower current conditions. Here, the arc resistances were too high for a reasonable number of meshes under very low current conditions. Therefore, a higher limit of resistance was set.

(4) FLIC-D In addition to FLIC-C, thermodynamic and transport properties of SF_6-PTFE mixed gas up to 10 MPa and 30000 K had been considered in the entire simulated area, instead of the multiplier only in the arcing area introduced in FLIC-B and -C. PTFE mass which has already been given in FLIC-A could flow in every area, therefore the program calculated mixture ratio of SF_6 and PTFE in every mesh. The program used tables of the properties obtained in Chapter 3, and derived corresponding values in each mesh.

5. Results of Gas Flow Simulations

Pressures at thermal puffers were observed to compare and discuss results. It is true that agreements of simulation results with measured values of the puffer pressure do not guarantee the accuracy or the reliability of the program. However, pressure is one of the relevant factors when evaluating performance and is easy to measure. Its advantage is the fact that they have always been measured in experiments or interruption tests. Therefore, comparing pressure values is an important and useful step when evaluating gas flow simulation programs for GCBs.

Fig. 7 shows simulated results of puffer pressures in a Hybrid-Puffer™ chamber [16][17] by FLIC-A. The puffer pressures by FLIC-A agreed quite well with experimental data, and were 20% higher at its peak. Fig. 8 shows the results in a self-blast type chamber for FLIC-A, -B, -C and -D. The results with FLIC-A were much lower than experimental data, and FLIC-B, -C, and -D indicated higher values than the former, respectively. FLIC-D agreed with experimental data best among the 4 approaches.

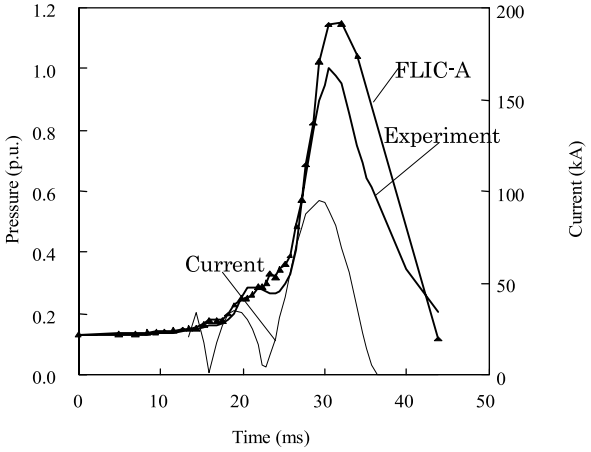

Fig. 7. Puffer-pressure in a Hybrid-Puffer chamber

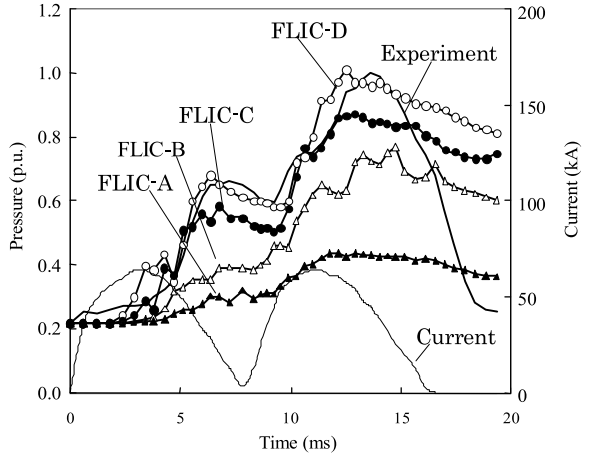

Fig. 8. Puffer-pressure in a self-blast type chamber

6. Evaluations of Considered Factors

All of the new methods introduced in FLIC-B, -C and -D contributed to obtaining a higher puffer pressure. The reason cannot be stated easily because the simulation did not consider linear cases, and the effects might appear as accumulations of many factors. However, it can be explained qualitatively as described below.

6.1 Thermodynamic and Transport Properties of High-pressure and -temperature SF_6-PTFE Gas

Comparing FLIC-A and -B, and FLIC-C and -D leads to the conclusion that the thermodynamic and transport properties of SF_6-PTFE gas are greatly affected by the gas pressure in the puffer chamber. Gas constants R shown in Fig. 2 are higher for higher ratios of PTFE. For example, R at 15000 K is 450 J/kg/K for 0% PTFE and 590 J/kg/K for 100% PTFE, which is 1.3 times. R affects pressure p proportionally at each mesh as shown in Eq. (23). Although there are both factors for increments and decrements of gas pressures, judging from the results in Fig. 8 and Eq. (23). The increments of R values could be the main factor increasing puffer pressure.

We can also conclude that consideration of the properties of SF_6-PTFE in all simulated area gives more accurate results than considering them only in the arcing area. This means that the diffusion of PTFE gas in the puffer chambers contributes to increasing pressure, and the mechanisms of the pressure rise are not only temperature rise or mass flow.

6.2 Conductivities and Diameters of Arcs The simulation results of FLIC-C are higher than that obtained by FLIC-B. This might be caused by temperature rises in the lower current region. In the simulation obtained by FLIC-B, the current flowed uniformly in the arcing area, even with a lower current, which made current density and pressure lower. On the other hand, with FLIC-C, the current concentrated toward the centre axis with a lower current. Therefore, even after peak current, temperatures within arcs remained high, which might produce a high pressure as derived by Eq. (23). Moreover, the arc voltages with FLIC-C are higher than the given constant values with FLIC-B in the lower current region. However, when the current became very low around current zero in FLIC-C, the arc diameter shrank and the gas flow through the nozzle throat around the arc differed, even though the arc maintained high temperature and pressure. This might be the reason why FLIC-C and FLIC-D indicated drops around time 9 ms, which agreed with experimental data very well.

6.3 Why Did FLIC-A Not Agree in the Self-blast Chamber ? There remains a question as to why FLIC-A did not agree with experimental data in self-blast type chambers while it was relatively useful in Hybrid-Puffer^{TM} type chambers. Fig. 9 shows examples of ratios of P_{SLF} (pressure in puffer chamber with SLF90% current interruption) against $P_{no\text{-}load}$ (that with no-load operation). The value of $P_{SLF}/P_{no\text{-}load}$ for a self-blast type chamber is twice of that of the Hybrid-Puffer^{TM} type. This suggests that the thermal energy in self-blast type chambers dominates the formation of puffer pressure with a high current interruption, while the Hybrid-Puffer^{TM} type still depends on mechanical compression. Therefore, it might not be mandatory to consider PTFE properties or arc diameter for Hybrid-Puffer^{TM} type chambers, and they might become necessary after featuring hot gas in self-blast type chambers. The literature [18] reports that multi-molecule simulations of pure SF_6 gas are much different from mono-molecule simulations in self-blast type chambers, while both simulation methods were not so different in puffer-type chambers. This phenomenon seems to be due to similar reasons.

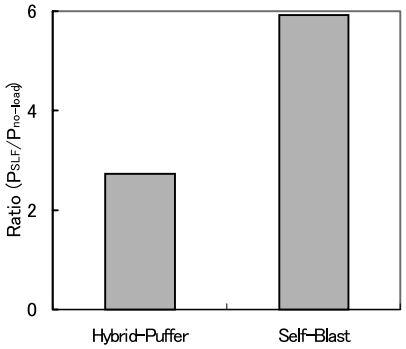

Fig. 9. Ratio of maximum puffer pressure in SLF90% interruption against that in no-load operation

7. Conclusions

This paper describes how taking account of thermodynamic and transport properties of SF_6-PTFE mixed gas in a large area in a simulated chamber is important for obtaining reasonable data in hot gas flow simulations for self-blast type chambers. This indicates that one of the important mechanisms of pressure rise in a self-blast type chamber is gas property along with temperature rise and mass contamination. Furthermore, taking account of arcing diameter according to the properties was one of the relevant factors. On the contrary, to simulate conventional puffer-type chambers, they were not so relevant and it could be unnecessary to consider the above, which might make a simulation simpler and faster. Users of hot gas flow simulations should select simulation methods carefully.

(Manuscript received Oct. 28, 2004)

References

(1) M. Okamoto, M. Ishikawa, K. Suzuki, and H. Ikeda: "Computer simulation of phenomena associated with hot gas in puffer-type gas circuit breaker", *IEEE Trans. Power Delivery*, Vol.6, pp.833–839 (1991-4)

(2) T. Mori, H. Ohashi, H. Mizoguchi, and K. Suzuki: "Investigation of technology of developing large capacity and compact size GCB", *IEEE Trans. Power Delivery*, Vol.12, pp.747–753 (1997-2)

(3) T. Shinkai, M. Ooi, T. Uchii, H. Kawano, T. Nakamoto, and H. Ikeda: "Gas density and temperature in thermal volume for self-blast interrupting chambers", Proc. of IEEE/PES T&D Conf. and Ex. 2002: Asia Pacific, Vol.1, pp.419–423 (2002)

(4) T. Mori, K. Iwamoto, T. Nakamoto, and K. Suzuki: "Development of gas flow simulation method considering ablation for GCB chambers", The Papers of Technical Meeting on Switching & Protecting Eng., IEE Japan, SP-99-86, pp.61–66 (1999) (in Japanese)

(5) H. Kawano, K. Iwamoto, N. Kato, Y. Tanaka, and T. Sakuta: "Gas flow simulation for GCB chambers by moving movable parts", The Papers of Technical Meeting on Switching & Protecting Eng., IEE Japan, SP-01-33, pp.57–62 (2001) (in Japanese)

(6) M. Claessens, K. Möller, and H.G. Thiel: "A computational fluid dynamics simulation of high- and low-current arcs in self-blast circuit breakers", *J. Phys. D, Appl. Phys.*, Vol.30, pp.1899–1907 (1997)

(7) S.D. Eby and J.Y. Trépanier: "Computation of the radiative transfer in SF_6

circuit-breaker arcs using the P-1 model of radiation", Proc. of 12th Int. Conf. on Gas Discharges and Their Applications, Vol.2, pp.570–573 (1997-9)
(8) A. Gleizes, M. Razafinimanana, and S. Vacquié: "Equilibrium composition thermodynamic properties and transport coefficients of SF_6-N_2 mixtures", Internal Report 40277-85-1, CNRS, EDF arc Electrique (1985-2)
(9) L.S. Frost and R.W. Liebermann: "Composition and transport properties of SF_6 and their use in a simplified enthalpy flow arc model", *Proc. IEEE*, Vol.59, pp.474–485 (1971-4)
(10) B. Chervy, A. Gleizes, and M. Razafinimanana: "Thermodynamic properties and transport coefficients in SF_6-Cu mixtures at temperatures of 300–30000 K and pressures of 0.1-1 MPa", *J. Phys. D, Appl. Phys*., Vol.27, pp.1193–1206 (1994)
(11) Y. Tanaka, K.C. Paul, and T. Sakuta: "Thermodynamic and Transport Properties of N_2/O_2 Mixtures at Different Admixture Ratios", *T. IEE Japan*, Vol.120-B, pp.24–30 (2000)
(12) K.C. Paul, T. Sakuta, and T. Takashima: "Transport and thermodynamic properties of SF_6 gas contaminated by PTFE reinforced with Al_2O_3 and BN particles", *IEEE Trans. Plasma Sci.*, Vol.25, pp.786–798 (1997)
(13) J.M. Yos: "Transport Properties of Nitrogen, Hydrogen, Oxygen, and Air to 30,000 K", Research and Advanced Development Division AVCO Corporation, Massachusetts, 1967, Amendments to AVCO RAD-TM-63-7
(14) P. Kovitya: "Thermodynamic and transport properties of ablated vapors of PTFE, alumina, perspex, and PVC in the temperature range 5000–30000 K", *IEEE Trans. Plasma Sci.*, Vol.PS-12, No.1, pp.38–42 (1984-3)
(15) P. Chévrier, M. Barrault, C. Fiéver, J. Maftoul, and J. Millon Frémillon: "Industrial applications of high-, medium- and low-voltage arc modelling", *J. Phys. D, Appl. Phys.*, Vol.30, pp.1346–1355 (1997)
(16) S. Yanabu, H. Mizoguchi, and M. Toyoda: "Development of novel hybrid interrupting chamber for gas circuit breaker utilizing self-pressure-rise phenomena by arc," *IEEE Trans. Power Delivery*, Vol.4, pp.355–361 (1989-1)
(17) T. Mori, H. Mizoguchi, N. Kato, and M. Toyoda: "Investigation of two types of interrupting chamber with low drive energy and development of 245-kV GCB", *IEEE Trans. Power Delivery*, Vol.10, pp.158–167 (2004-1)
(18) N. Osawa and Y. Yoshioka: "The calculation method of puffer pressure in gas circuit breaker taking decomposition gas effect into consideration", *IEEJ Trans. PE*, Vol.123, No.8, pp.1002–1010 (2003-8)

Tadashi Mori (Member) was born in Aichi Prefecture, Japan, on June 14, 1966. He received his B.S. and M.S. degrees in electrical engineering from Nagoya University, Nagoya, Japan, in 1989 and 1991, respectively. Currently, he is with Toshiba Corporation, Kawasaki where he joined in 1991. He has been engaged in the development of gas-insulated switchgears and the study of interruption phenomena. He was with TMT&D Corporation from 2002 to 2005. Mr. Mori is a member of the IEEE.

Katsuharu Iwamoto (Non-member) was born in Yamaguchi, Japan, on September 15, 1948. He received B.S., M.S. and Ph.D. degrees in mechanical engineering from Kyushu University in 1971, 1973 and 1996 respectively. Currently, he is with Toshiba Corporation, Kawasaki where he joined in 1973. He was first engaged in a development of a steam turbine. Then he has worked on gas flow analysis and measurements in gas circuit breakers. He was with TMT&D Corporation from 2002 to 2005. Dr. Iwamoto is a member of the Japan Society of Mechanical Engineers, the Japan Society of Applied Physics and the Optical Society of America.

Hiromichi Kawano (Member) was born in Oita Prefecture, Japan, on March 7, 1961. He received his B.S. and M.S. degrees in electrical engineering from Kyoto University, Kyoto, Japan, in 1983 and 1985, respectively. Currently, he is a Manager of the High Power Technology Group, Toshiba Corporation, Kawasaki where he joined in 1985. He has been engaged in the development and design of gas-insulated switchgears and the study of interruption phenomena. He was with TMT&D Corporation from 2002 to 2005. Mr. Kawano is a member of the IEEE.

Yasunori Tanaka (Member) was born in Japan on November 19, 1970. He received the B.S., M.S. and Ph.D. degrees in electrical engineering from Nagoya University, Japan in 1993, 1995 and 1998 respectively. He has been working as a Research Associate and then as an Associate Professor in the Department of Electrical and Electronic Engineering, Kanazawa University, Kanazawa, Japan since April 1998. His research interests include the arc interruption phenomena and thermal plasma applications.

◇ ◇ ◇

◇ ◇ ◇